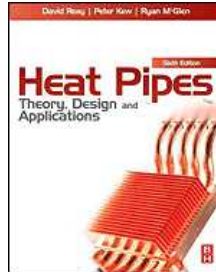


Chapters *To Go*



Heat Pipes: Theory, Design and Applications, Sixth Edition

by D.A. Reay, P.A. Kew and R.J. McGlen

Elsevier Science and Technology Books, Inc.. (c) 2014. Copying Prohibited.

Reprinted for Aaron Scott, NASA

aaron.m.scott@nasa.gov

Reprinted with permission as a subscription benefit of **Skillport**,

All rights reserved. Reproduction and/or distribution in whole or in part in electronic, paper or other forms without written permission is prohibited.



Chapter 4: Design Guide

4.1 INTRODUCTION

The design of a heat pipe or thermosyphon to fulfil a particular duty involves four broad processes:

1. Selection of appropriate type and geometry
2. Selection of candidate materials
3. Evaluation of performance limits
4. Evaluation of the actual performance

The background to each of these stages is covered in Chapters 2 and 3. In this chapter, the theoretical and practical aspects are discussed with reference to sample design calculations.

4.2 HEAT PIPES

The design procedure for a heat pipe is outlined in [Fig. 4.1](#).

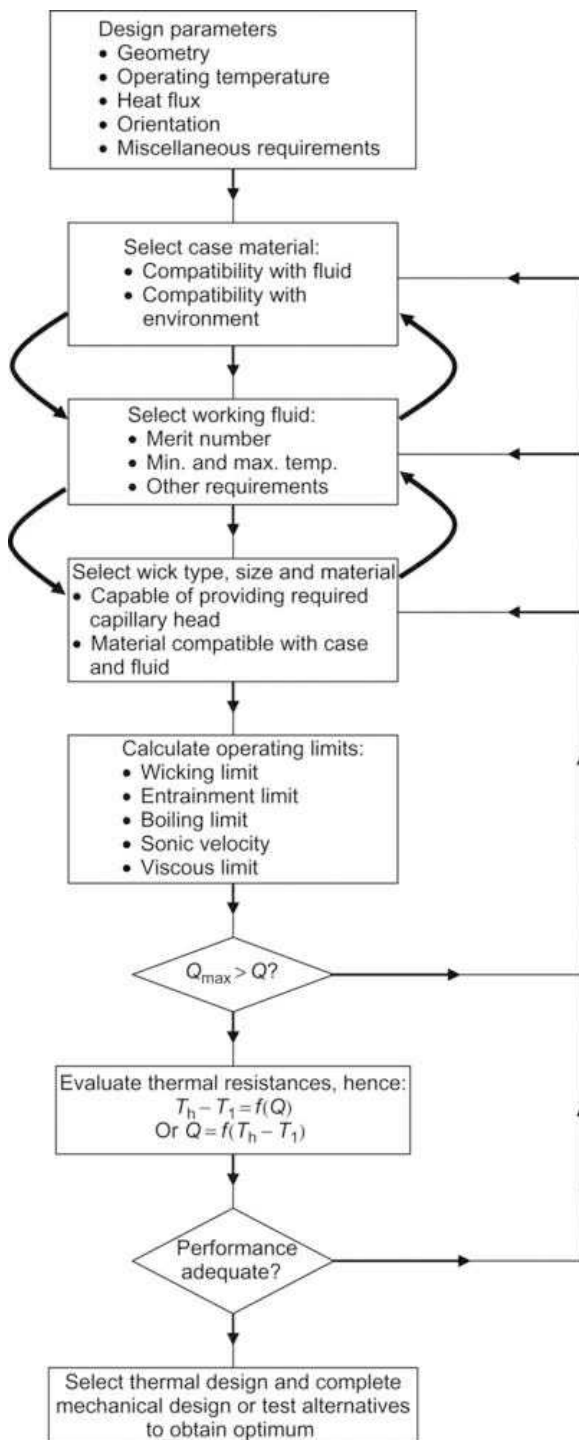


Figure 4.1: Flow sheet for heat pipe design

As with any design process, many of the decisions that must be taken are interrelated and the process is iterative. For example, choice of the wick and case material eliminates many candidate working fluids (often including water) due to compatibility constraints. If the design then proves inadequate with the available fluids, it is necessary to reconsider the choice of construction materials.

Two aspects of practical design, which must also be taken into consideration, are the fluid inventory and performance at off-design conditions, particularly during the start-up of the heat pipe.

4.2.1 Fluid Inventory

A feature of heat pipe design, which is important when considering small heat pipes and units for space use, is the working fluid inventory. It is a common practice to include a slight excess of working fluid over and above that required to saturate the wick, but when the vapour space is of small volume a noticeable temperature gradient can exist at the condenser, similar to

that which would be observed if a noncondensable gas was present. This reduces the effective length of the condenser, hence impairing heat pipe performance. Another drawback of excess fluid is peculiar to heat pipes in space, i.e. in zero gravity the fluid can move about the vapour space, affecting the dynamics of the spacecraft.

If there is a deficiency of working fluid, the heat pipe may fail because of the inability of any artery to fill. This is not so critical with homogeneous wicks as some of the pores will still be able to generate capillary action. Marcus [1] discusses in detail these effects and the difficulties encountered in ensuring whether the correct amount of working fluid is injected into the heat pipe. One way of overcoming the problem is to provide an excess fluid reservoir, which behaves as a sponge, absorbing working fluid that is not required by the primary wick structure.

4.2.2 Priming

With heat pipes having some form of arterial wick, it is necessary to ensure that should an artery become depleted of working fluid, it should be able to refill automatically. It is possible to calculate the maximum diameter of an artery to ensure that it will be able to reprime. The maximum priming height that can be achieved by a capillary is given by the equation:

$$(4.1) \quad h + h_c = \frac{\sigma_1 \cos \theta}{(\rho_l - \rho_v)g} \times \left(\frac{1}{r_{p1}} + \frac{1}{r_{p2}} \right)$$

where h is the vertical height to the base of the artery, h_c the vertical height to the top of the artery, r_{p1} the first principal radius of curvature of the priming meniscus, and r_{p2} is the second principal radius of curvature of the priming meniscus.

For the purpose of priming, the second principal radius of curvature of the meniscus is extremely large (approximately $1/\sin \phi$). For a cylindrical artery,

$$h_c = d_a$$

and

$$r_{p1} = \frac{d_a}{2}$$

where d_a is the artery diameter.

Hence the above equation becomes:

$$(4.2) \quad h + d_a = \frac{2\sigma_1 \cos \theta}{(\rho_l - \rho_v)g \times d_a}$$

which produces a quadratic in d_a that may be solved as:

$$(4.3) \quad d_a = \frac{1}{2} \left[\left(\sqrt{h^2 + \frac{8\sigma_1 \cos \theta}{(\rho_l - \rho_v)g}} \right) - h \right]$$

An artery can deprime when vapour bubbles become trapped in it. It may be necessary to reduce the heat load in such circumstances, to enable the artery to reprime. It is possible to design a heat pipe incorporating a tapered artery effectively, a derivative of the monogroove wick system illustrated in Fig. 3.7. Use of this design [2] facilitated bubble venting into the vapour space and achieved significant performance improvements.

4.3 DESIGN EXAMPLE 1

4.3.1 Specification

A heat pipe is required which will be capable of transferring a minimum of 15 W at a vapour temperature between 0°C and 80°C over a distance of 1 m in zero gravity (a satellite application). Constraints on the design are such that the evaporator and condenser sections are each to be 8 cm long, located at each end of the heat pipe, and the maximum permissible temperature drop between the outside wall of the evaporator and the outside wall of the condenser is 6°C. Because of weight and volume limitations, the cross-sectional area of the vapour space should not exceed 0.197 cm². The heat pipe must also withstand bonding temperatures.

Design a heat pipe to meet this specification.

4.3.2 Selection of Materials and Working Fluid

The operating conditions are contained within the specification. The selection of wick and wall materials is based on the criteria discussed in Chapter 3. As this is an aerospace application, low mass is an important factor.

On this basis, aluminium alloy 6061 (HT30) is chosen for the wall and stainless steel for the wick.

If it is assumed that the heat pipe will be of a circular cross section, the maximum vapour space area of 0.197 cm^2 yields a radius of 2.5 mm.

Working fluids compatible with these materials, based on available data, include:

- Freon 11
- Freon 113
- Acetone
- Ammonia

Water must be dismissed at this stage, both on compatibility grounds and because of the requirement for operation at 0°C with the associated risk of freezing. Note that the freon refrigerants are CFCs and are no longer available, but are included in the evaluation in order to demonstrate the properties of a range of fluids.

The operating limits for each fluid must now be examined.

4.3.2.1 Sonic Limit

The minimum axial heat flux due to the sonic limitation will occur at the minimum operating temperature, 0°C , and can be calculated from Eq. (2.58) with the Mach number set to unity.

$$\dot{q}_s = \rho_s L \sqrt{\frac{\gamma R T_v}{2(\gamma + 1)}}$$

The gas constant for each fluid may be obtained from,

$$R = \frac{R_o}{\text{Molecular weight}} = \frac{8315}{M_w} \text{ J/kg K}$$

For ammonia, $\gamma=1.4$ [3] and its molecular weight is 31, the latent heat and density may be obtained from Appendix 1, therefore \dot{q}_s is given by:

$$\begin{aligned} \dot{q}_s &= 3.48 \times 1263 \times \sqrt{\frac{1.4}{2(1.4 + 1)} \frac{8315 \times 273}{31}} = 84 \times 10^7 \text{ W/m}^2 \\ &= 84 \text{ kW/cm}^2 \end{aligned}$$

Similar calculations may be carried out for the other candidate fluids, yielding

Freon 11	0.69 kW/cm ²
Freon 113	3.1 kW/cm ²
Acetone	1.3 kW/cm ²
Ammonia	84 kW/cm ²

Since the required axial heat flux is $15/0.197 \text{ W/cm}^2 \approx 0.076 \text{ kW/cm}^2$, the sonic limit would not be encountered for any of the candidate fluids.

It is worth noting that the term $\sqrt{\gamma/(\gamma+1)}$ varies from 0.72 to 0.79 for values of γ from 1.1 to 1.66; therefore, when the sonic limit is an order of magnitude above the required heat flux it is not essential that γ be known precisely for the fluid.

4.3.2.2 Entrainment Limit

The maximum heat transport due to the entrainment limit may be determined from Eq. (2.62):

$$\dot{q} = \sqrt{\frac{2\pi\rho_v L^2 \sigma_1}{z}}$$

which may be written as:

$$\dot{Q}_{em} = \pi r_v^2 L \sqrt{\frac{2\pi\rho_v \sigma_1}{z}}$$

where z is the characteristic dimension of the liquid–vapour interface for a fine mesh that may be taken as 0.036 mm. The entrainment limit is evaluated at the highest operating temperature.

The properties of the fluids and the resulting entrainment limits are given in [Table 4.1](#).

Table 4.1: Properties of Candidate Fluids at 80°C

Fluid	L (kJ/kg)	σ_1 (mN/m)	ρ_v (kg/m ³)	\dot{Q}_{em} (kW)
Freon 11	221	10.7	27.6	0.98
Freon 113	132	10.6	18.5	0.48
Acetone	495	16.2	4.05	1.04
Ammonia	891	7.67	34	3.75

A sample calculation for acetone is reproduced below.

Particular care must be taken to ensure that the units used are consistent.

$$L = \text{J/kg} \quad \sigma_1 = \text{N/m} \quad \rho_v = \text{kg/s} \quad r_v = \text{m (or } A = \text{m}^2) \quad z = \text{m}$$

Some useful conversion factors are given in Appendix 1.

Then we have:

$$\begin{aligned} \text{m}^2 \times \frac{\text{J}}{\text{kg}} \times \sqrt{\frac{\text{kg N}}{\text{m}^3 \text{m}}} &= \text{m}^2 \times \frac{\text{J}}{\text{kg}} \times \sqrt{\frac{\text{kg kg} \times \text{m}}{\text{m}^3 \text{m} \times \text{s}^2 \text{m}}} = \frac{\text{J}}{\text{s}} = \text{W} \\ \dot{Q}_{em, \text{acetone}} &= \pi r_v^2 L \sqrt{\frac{2\pi\rho_v \sigma_1}{z}} = \pi \times (2.5 \times 10^{-3})^2 \times 495 \\ &\quad \times 10^3 \sqrt{\frac{2\pi \times 4.05 \times 0.0162}{0.036 \times 10^{-3}}} = 1040 \text{ W} \end{aligned}$$

4.3.2.3 Wicking Limit

At this stage the wick was still to be specified, but a qualitative comparison of the potential performance of the four fluids can be obtained by evaluating the merit number:

$$\rho_l \frac{\sigma_1 L}{\mu_l}$$

for each fluid over the temperature range ([Fig. 4.2](#)).

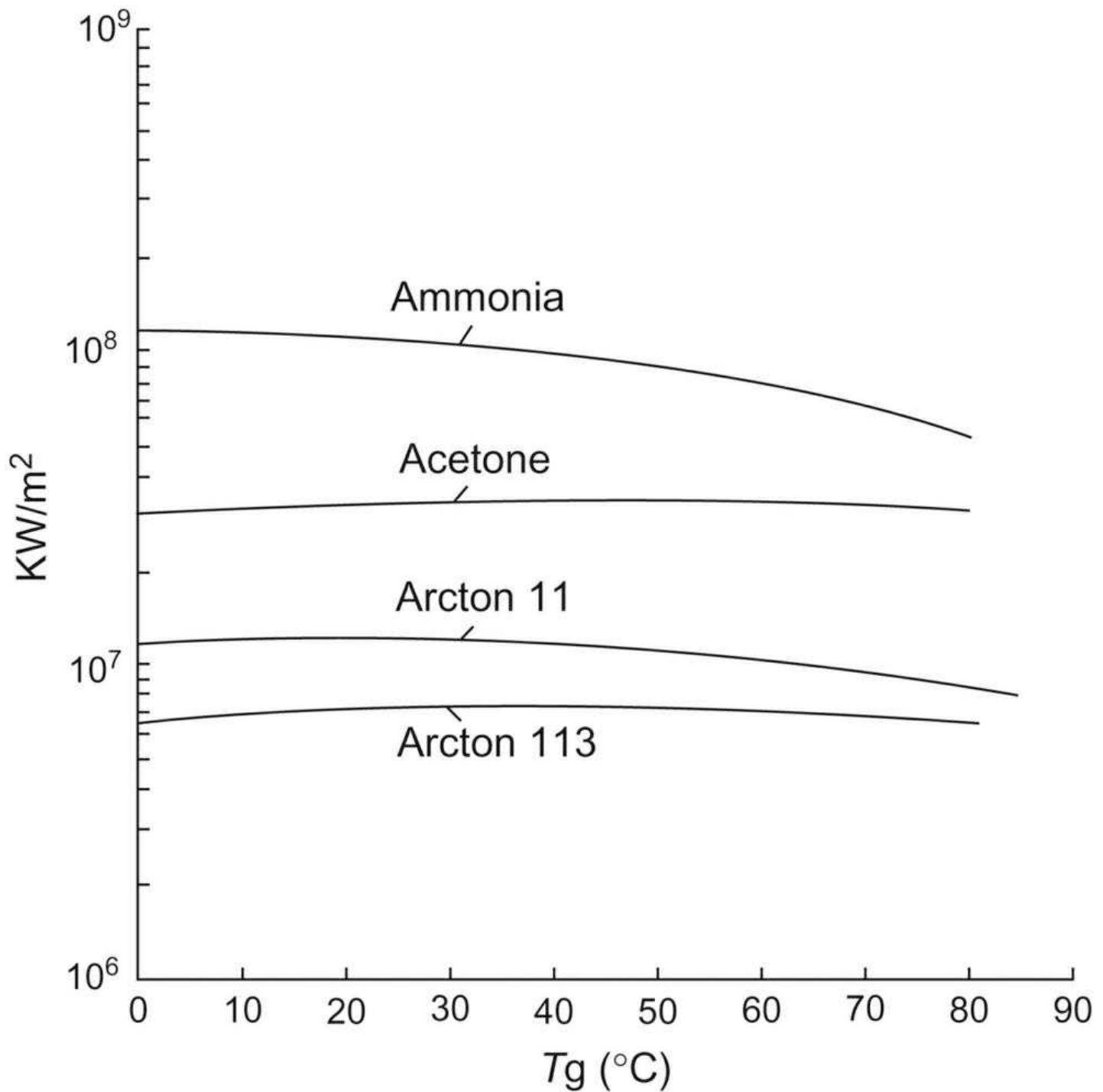


Figure 4.2: Merit number for candidate fluids

4.3.2.4 Radial Heat Flux

Boiling in the wick may result in the vapour blocking the supply of liquid to all parts of the evaporator. In arterial heat pipes, bubbles in the artery itself can create even more serious problems. It is therefore desirable to have a working fluid with a high superheat ΔT to reduce the chance of nucleation. The degree of superheat to cause nucleation is given by:

$$\Delta T = \frac{3.06 \sigma_1 T_{\text{sat}}}{\rho_v L \delta}$$

where δ is the thermal layer thickness, and taking a representative value of 15 μm allows comparison of the fluids. ΔT is evaluated at 80°C, as the lowest permissible degree of superheat will occur at the maximum operating temperature. These are:

Freon 11	0.13 K
----------	--------

Freon 113	0.31 K
Acetone	0.58 K
Ammonia	0.02 K

These figures suggest that the freons and ammonia require only very small superheat temperatures at 80°C to cause boiling. Acetone is the best fluid from this point of view.

4.3.2.5 Priming of the Wick

A further factor in fluid selection is the priming ability (see [Section 4.2.2](#)). A comparison of the priming ability of fluids may be obtained from the ratio σ_f/ρ_l , and this is plotted against vapour temperature in [Fig. 4.3](#).

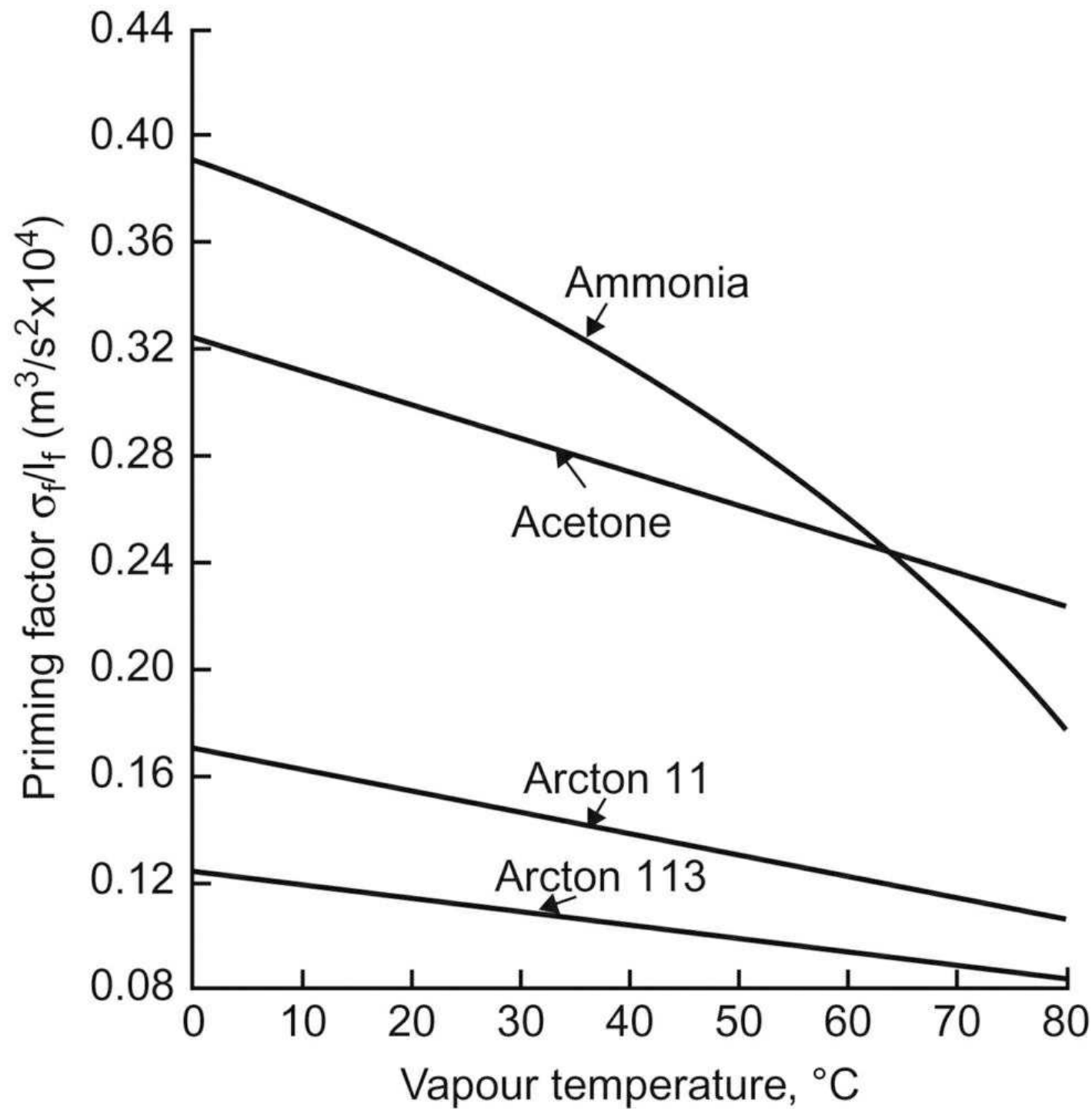


Figure 4.3: Priming factor for selected fluids

Acetone and ammonia are shown to be superior to the freons over the whole operating temperature range.

4.3.2.6 Wall Thickness

The requirement of this heat pipe necessitates the ability to be bonded to a radiator plate. Depending on the type of bonding used, the heat pipe may reach 170°C during bonding, and therefore vapour pressure is important in determining the wall thickness.

At this temperature, the vapour pressures of ammonia and acetone are 113 and 17 bar, respectively. Taking the 0.1% proof stress, Ω , of HT30 aluminium as 46.3 MN/m² (allowing for some degradation of properties in weld regions), and using the thin cylinder formula,

$$t = \frac{Pr}{\Omega}$$

the minimum wall thickness for ammonia is 0.65 and 0.1 mm for acetone. There is therefore a mass penalty attached to the use of ammonia.

4.3.2.7 Conclusions on Selection of Working Fluid

Acetone and ammonia both meet the heat transport requirements, ammonia being superior to acetone in this respect. Nucleation occurs more readily in an ammonia heat pipe, and the pipe may also be heavier. The handling of ammonia to obtain high purity is difficult, and the presence of any water in the working fluid may lead to long-term degradation in performance.

Acetone is therefore selected in spite of the somewhat inferior thermal performance.

4.3.3 Detail Design

4.3.3.1 Wick Selection

Two types of wick structure are proposed for this heat pipe, homogeneous and arterial types. A homogeneous wick may be a mesh, twill or felt, and arterial types normally incorporate a mesh to distribute liquid circumferentially.

Homogeneous meshes are easy to form but have inferior properties to arterial types. The first question is, therefore, will a homogeneous wick transport the required amount of fluid over 1 m to meet the heat transport specification?

To determine the minimum flow area to transport 15 W, one can equate the maximum capillary pressure to the sum of the liquid and gravitational pressure drops (neglecting vapour ΔP).

$$\Delta P_l + \Delta P_g = \Delta P_c$$

where

$$\Delta P_c = \frac{2\sigma_l \cos \theta}{r_e}$$

$$\Delta P_l = \frac{\mu_l \dot{Q} l_{\text{eff}}}{\rho_l L A_w K}$$

$$\Delta P_g = \rho_l g h$$

The gravitational effect is zero in this application, but is included to permit testing of the heat pipe on the ground. The value of h may be taken as 1 cm based on end-to-end tilt plus the tube diameter. The effective length l_{eff} is 1 m and $\cos \theta$ is taken to be unity.

The effective capillary radius for the wick is 0.029 mm; therefore, using the surface tension of acetone at 80°C,

$$\Delta P_c = \frac{2\sigma_l \cos \theta}{r_e} = \frac{2 \times 0.0162 \times 1}{0.029 \times 10^{-3}} = 1120 \text{ N/m}^2$$

The wick permeability, K , is calculated using the Blake–Koseny equation:

$$K = \frac{d_w^2 (1 - \varepsilon)^3}{66.6 \varepsilon^2}$$

where ε is the volume fraction of the solid phase (0.314) and d_w the wire diameter (0.025 mm).

$$K = \frac{(2.5 \times 10^{-5})^2 (1 - 0.314)^3}{66.6 \times 0.314^2} = 3 \times 10^{-11}$$

Therefore, considering the properties of acetone at 80°C,

$$\begin{aligned}\rho_l &= 719 \text{ kg/m}^3 \\ \mu_l &= 0.192 \text{ cP} = 192 \times 10^{-6} \text{ kg/ms or Ns/m}^2 \\ \Delta P_l &= \frac{\mu_l \dot{Q}_{\text{eff}}}{\rho_l L A_w K} = \frac{192 \times 10^{-6} \times 15 \times 1}{719 \times 495 \times 10^3 \times 3 \times 10^{-11} A_w} \\ &= \frac{0.027}{A_w} \text{ N/m}^2\end{aligned}$$

The gravitational pressure is:

$$\Delta P_g = \rho_l g h = 719 \times 9.81 \times 0.01 = 70 \text{ N/m}^2$$

Equating the three terms gives:

$$\begin{aligned}\Delta P_l + \Delta P_g &= \Delta P_c \\ \frac{0.027}{A_w} + 70 &= 1120 \\ A_w &= \frac{0.027}{1120 - 70} = 26 \times 10^{-6} \text{ m}^2 \equiv 0.26 \text{ cm}^2\end{aligned}$$

Since the required wick area (0.26 cm²) is greater than the available vapour space area (0.197 cm²), it can be concluded that the homogeneous type of wick is not acceptable. An arterial wick must be used.

4.3.3.2 Arterial Diameter

[Equation \(4.3\)](#) above, and reproduced below, describes the artery priming capability, setting a maximum value on the size of any arteries:

$$d_a = \frac{1}{2} \left[\sqrt{\left(h^2 + \frac{8 \sigma_l \cos \theta}{(\rho_l - \rho_v) g} \right)} - h \right]$$

Using this equation, d_a is evaluated at a vapour temperature of 20°C (for convenience priming ability may be demonstrated at room temperature), and h is taken as 1 cm to cater for arteries near the top of the vapour space.

$$\begin{aligned}d_a &= \frac{1}{2} \left[\sqrt{\left(0.01^2 + \frac{8 \times 0.0237 \times 2}{(790 - 0.64) \times 9.81} \right)} - 0.01 \right] \\ &= 0.58 \times 10^{-3} \text{ m}\end{aligned}$$

Thus, the maximum permitted value is 0.58 mm. To allow for uncertainties in fluid properties, wetting (θ assumed 0°) and manufacturing tolerances, a practical limit is 0.5 mm.

4.3.3.3 Circumferential Liquid Distribution and Temperature Difference

The circumferential wick is the most significant thermal resistance in this heat pipe, and its thickness is limited by the fact that the temperature drop between the vapour space and the outside surface of the heat pipe and vice versa should be 3°C maximum. Assuming that the temperature drop through the aluminium wall is negligible, the thermal conductivity of the wick may be determined and used in the steady state conduction equation.

$$k_{\text{wick}} = \left(\frac{\beta - \varepsilon}{\beta + \varepsilon} \right) k_l$$

where

$$\beta = \left(1 - \frac{k_s}{k_1}\right) / \left(1 - \frac{k_s}{k_1}\right)$$

$$k_s = 16 \text{ W/m}^\circ\text{C (steel)}$$

$$k_1 = 0.165 \text{ W/m}^\circ\text{C (acetone)}$$

$$\therefore \beta = \frac{1 + 97}{1 - 97} = -1.02$$

The volume fraction ε of the solid phase is approximately 0.3:

$$\therefore k_{\text{wick}} = \left(\frac{-1.02 - 0.3}{-1.02 + 0.3} \right) \times 0.165$$

$$= 0.3 \text{ W/m}^\circ\text{C}$$

Using the basic conduction equation:

$$\dot{Q} = kA_e \frac{\Delta T}{t}$$

$$t = \frac{kA_e \Delta T}{\dot{Q}}$$

where A_e is the area of the evaporator (8 cm long, 0.5 cm diameter) and \dot{Q} is the required heat load.

$$t = \frac{0.3 \times 3 \times \pi \times 5 \times 10^{-3} \times 80 \times 10^{-3}}{15}$$

$$= 75 \times 10^{-6} \text{ m} \equiv 0.075 \text{ mm}$$

Thus, the circumferential wick must be 400 mesh, which has a thickness of 0.05 mm. Coarser meshes are too thick, resulting in unacceptable temperature differences across the wick in the condenser and evaporator.

4.3.3.4 Arterial Wick

Returning to the artery, the penultimate section revealed that the maximum artery depth permissible was 0.5 mm. In order to prevent nucleation in the arteries, they should be kept away from the heat pipe wall and formed of low conductivity material. It is also necessary to cover the arteries with a fine pore structure and 400-mesh stainless steel is selected. It is desirable to have several arteries to give a degree of redundancy, and two proposed configurations are considered, one having six arteries as shown in [Fig. 4.4](#), and the other having four arteries. In the former case, each groove is nominally 1.0-mm wide, and in the latter case, 1.5 mm.

Machined stainless steel former

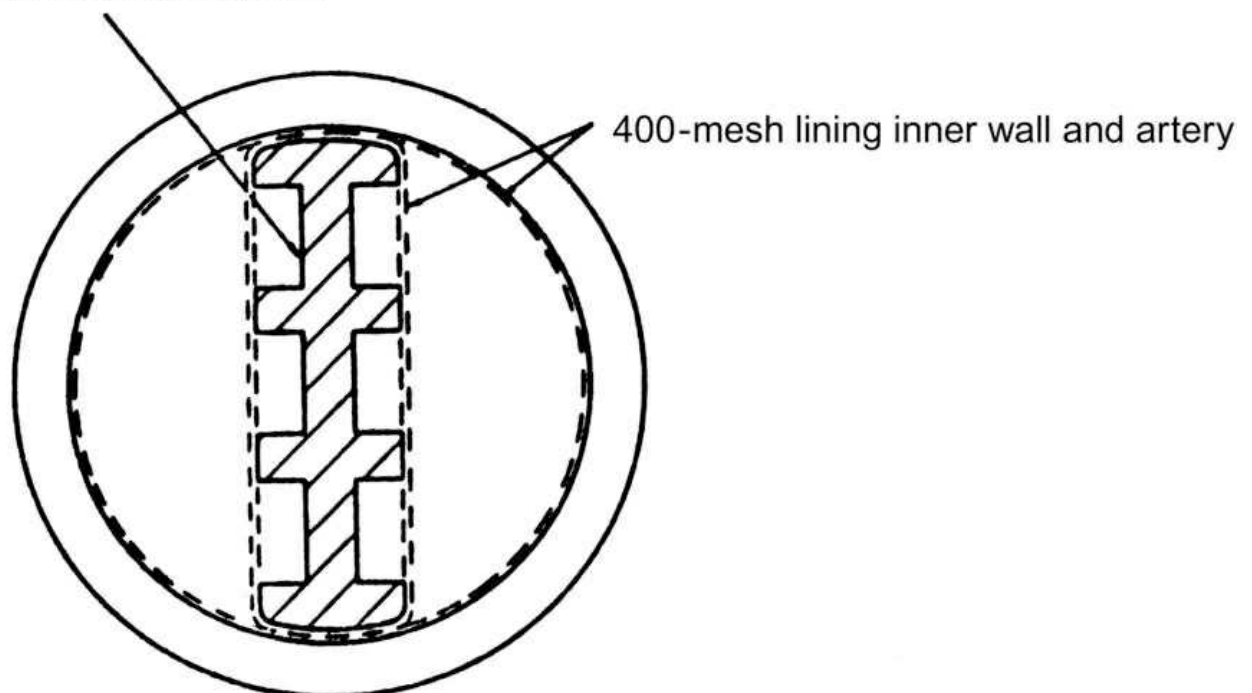


Figure 4.4: Design of wick

4.3.3.5 Final Analysis

It is now possible to predict the overall capability of the heat pipe, to check that it meets the specification.

We have already shown that entrainment and sonic limitations will not be exceeded and that the radial heat flux is acceptable. The heat pipe should also meet the overall temperature drop requirement, and the arteries are sufficiently small to allow repriming at 20°C. The wall thickness requirement for structural integrity (0.1 mm minimum) can easily be satisfied. The wicking limitation will therefore determine the maximum performance.

$$\text{i.e. } \Delta P_{la} + \Delta P_{lm} + \Delta P_g + \Delta P_v = \Delta P_c$$

where ΔP_{la} is the pressure drop in the artery and ΔP_{lm} the loss in the circumferential wick.

The axial flow in the mesh will have little effect and can be neglected. McAdams [4] presents an equation for the pressure loss, assuming laminar flow, in a rectangular duct, and shows that the equation is in good agreement with experiment for streamline flow in rectangular ducts having depth/width ratios, a_d/b_d of 0.05–1.0.

This equation may be written as:

$$\Delta P_{la} = \frac{4K_l \times l_{\text{eff}} Q}{a_d^2 b_d^2 \theta_c N}$$

where N is the number of channels, θ_c a function of channel aspect ratio and is given in Fig. 4.5 and

$$K_l = \frac{\mu_l}{\pi \eta L}$$

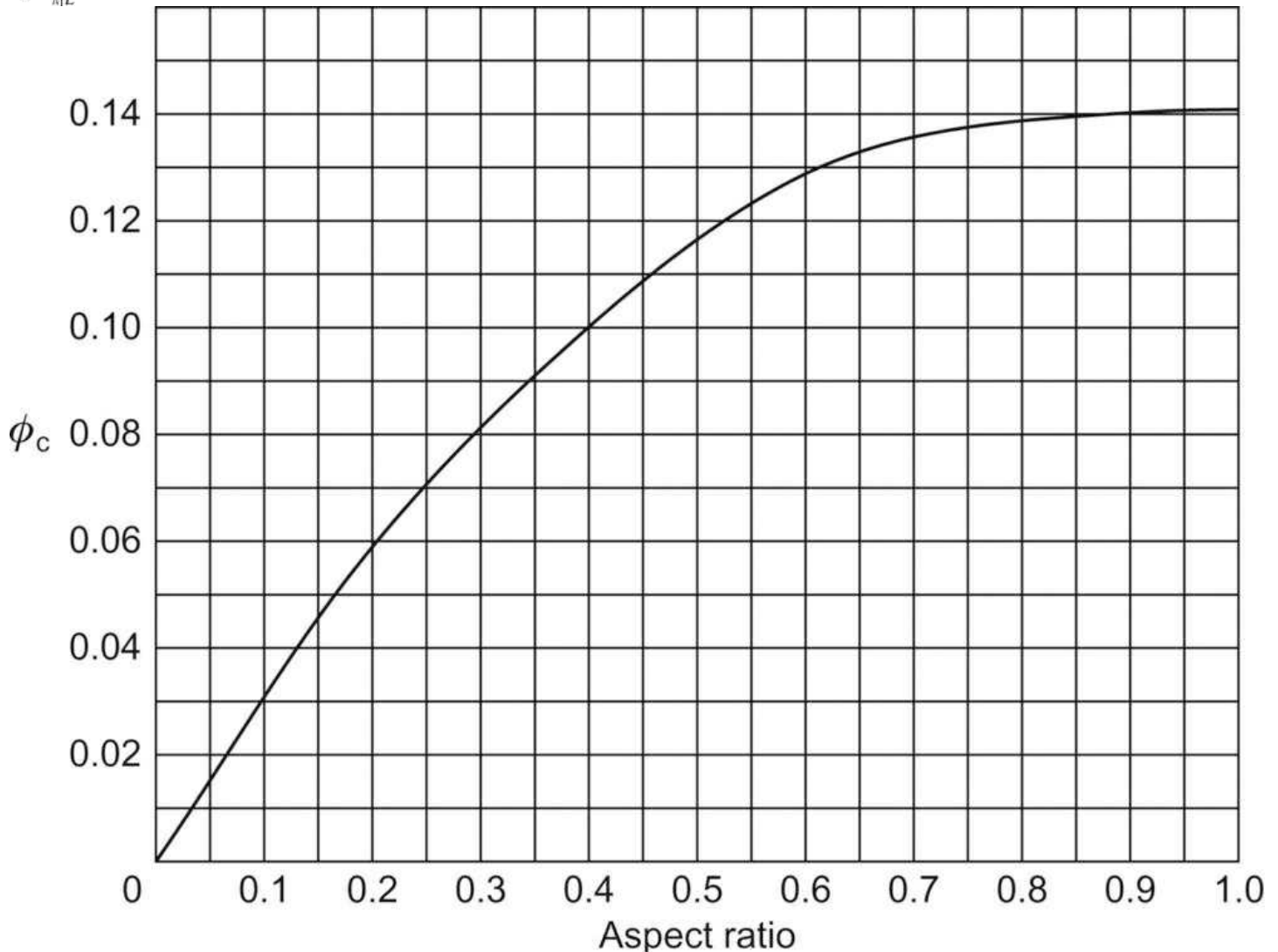


Figure 4.5: Channel aspect ratio factor

The summed pressure loss in the condenser and evaporator is given by:

$$\Delta P_{la} = \frac{K_l \times l_{eff} \times Q}{2K A_c}$$

where l_{eff} is the effective circumferential flow length approximately equal to

$$\frac{\pi r_w}{4} \text{ carrying } \frac{\dot{m}}{4}$$

where \dot{m} is the liquid mass flow, A_c the circumferential flow area (mesh thickness \times condenser or evaporator length) and K the permeability of 400 mesh.

The circumferential flow area for 400 mesh with two layers is

$$A_c = 8 \times 10^{-2} \times 0.1 \times 10^{-3} \text{ m}^2 = 8 \times 10^{-6} \text{ m}^2$$

A resistance occurs in both the evaporator and the condenser, therefore; substituting in the above equation:

$$\begin{aligned} \Delta P_{lm} &= \frac{\pi \times 2.5 \times 10^{-3}}{2 \times 4} \frac{1}{8 \times 10^{-6}} \frac{K_l Q}{0.314 \times 10^{-10}} \\ &= 4.00 \times 10^{12} K_l Q \text{ for each section} \\ \Delta P_{la} &= \frac{4 \times 0.92 \times K_l \times Q \times 10^{12}}{(0.5)^2 (1)^2 \times 0.115 \times 6} \\ &= 21.3 \times 10^{12} K_l Q \text{ for six channels} \\ &= \frac{4 \times 0.92 \times K_l \times Q \times 10^{12}}{(0.5)^2 (1.5)^2 \times 0.088 \times 4} \\ &= 18.59 \times 10^{12} K_l Q \text{ for four channels} \end{aligned}$$

The vapour pressure loss, which occurs in two near-semicircular ducts, can be obtained using the Hagen–Poiseuille equation if the hydraulic radius is used.

$$\Delta P_v = \frac{1}{2} \left\{ \frac{8 K_v l_{eff} Q}{\pi r_{H1}^4} \right\}$$

where

$$K_v = \frac{\mu_v}{\rho_v L}$$

Now the axial Reynolds number Re_z is given by:

$$Re_z = \frac{Q}{\pi r_{H1} \mu L}$$

The transitional heat load at which the flow becomes turbulent can be calculated assuming that transition from laminar to turbulent flow occurs at $Re_z=1000$, based on hydraulic radius (corresponding to 2000 if the Reynolds number is based on the diameter). Restricting the width of the stainless steel former in [Fig. 4.4](#) to 1.5 mm, $r_H=1.07$ mm.

\dot{Q} may be evaluated at the transition point using values of μ_v and L at several temperatures between 0°C and 80°C, as given below:

Vapour Temperatures (°C)	Transitional Load (W)
0	31.1
20	31.2
40	30.6
60	30.2
80	30.0

The transitional load is always greater than the design load of 15 W, but as the heat pipe may be capable of operating in excess of the design load, it is necessary to investigate the turbulent regime.

For $Re_z > 100$ and for two ducts:

$$\Delta P_v = \frac{0.00896 \mu_v^{0.25} Q^{1.75} l_{\text{eff}}}{2 \rho_v r_{11}^{1.75} L^{1.75}}$$

This is the empirical Blasius equation.

$$\begin{aligned} \Delta P_v(\text{laminar}) &= \frac{1}{2} \left(\frac{8 \times 0.92 K_v \times Q \times 10^{12}}{p \times 1.07^4} \right) \\ &= 0.9 \times 10^{12} K_v \times Q \\ \Delta P_v(\text{turbulent}) &= \frac{0.00896 \times 0.92}{2 \times (1.07 \times 10^{-3})^{4.75}} Q^{1.75} \left(\frac{m_v^{0.25}}{L^{1.75} r_v} \right) \\ &= 0.53 \times 10^{12} Q^{1.75} \left(\frac{m_v^{0.25}}{L^{1.75} r_v} \right) \end{aligned}$$

The gravitational pressure drop is:

$$\begin{aligned} \Delta P_g &= \rho_l g l \sin \phi \\ &= 0.0981 \rho_l l \end{aligned}$$

taking $l \sin \phi = 1 \text{ cm}$

The capillary pressure generated by the arteries is given by:

$$\begin{aligned} \Delta P_c &= \frac{2 \sigma_l \cos \theta}{r_c} \\ &= \frac{2}{0.003 \times 10^{-2}} \sigma_l \cos \theta \\ &= 0.667 \times 10^{-5} \sigma_l \end{aligned}$$

Summarising

$$\begin{aligned} \Delta P_c &= 0.667 \times 10^{-5} \sigma_l \\ \Delta P_g &= 0.0981 \rho_l \\ \Delta P_{vl} &= 0.9 \times 10^{12} K_v Q \\ \Delta P_{vt} &= 0.53 \times 10^{12} Q^{1.75} \left(\frac{\mu_v^{0.25}}{L^{1.75} \rho_v} \right) \\ \Delta P_{lm} &= 4 \times 10^{12} K_l Q \\ \Delta P_{la} &= 21.3 \times 10^{12} K_l Q \quad (\text{six channels}) \\ &= 18.59 \times 10^{12} K_l Q \quad (\text{four channels}) \end{aligned}$$

These equations involve \dot{Q} and the properties of the working fluid. Using properties at each temperature (in 20°C increments) over the operating range, the total capability can be determined as:

$$\begin{aligned} \Delta P_c &= \Delta P_{lm} + \Delta P_{la} \begin{cases} \text{six channels} \\ \text{four channels} \end{cases} \\ &+ \Delta P_g + \Delta P_v \begin{cases} \text{laminar} \\ \text{turbulent} \end{cases} \end{aligned}$$

This yields the following results:

Vapour Temperatures (°C)	Q (W)			
	Laminar Four Channels	Laminar Six Channels	Turbulent Four Channels	Turbulent Six Channels
0	21.6	20.9	—	—
20	34.0	32.5	22.6	22.0
40	42.6	40.2	27.9	27.0
60	49.1	45.8	33.0	32.0
80	51.4	47.6	36.4	35.0

In this example, it is assumed that the maximum resistance to heat transfer is across the wick, the other thermal resistances have not been calculated explicitly.

This heat pipe was constructed with six grooves in the artery structure and met the specification.

4.4 DESIGN EXAMPLE 2

4.4.1 Problem

Estimate the liquid flow rate and heat transport capability of a simple water heat pipe operating at 100°C having a wick of two layers of 250 mesh against the inside wall. The heat pipe is 30 cm long and has a bore of 1 cm diameter. It is operating at an inclination to the horizontal of 30°, with the evaporator above the condenser.

It will be shown that the capability of the above heat pipe is low. What improvement will be made if two layers of 100 mesh are added to the 250-mesh wick to increase liquid flow capability?

4.4.2 Solution – Original Design

The maximum heat transport in a heat pipe at a given vapour temperature, if governed by the wicking limit, may be obtained from the equation:

$$Q_{\max} = \dot{m}_{\max} L$$

where \dot{m}_{\max} is the maximum liquid flow rate in the wick.

Using the standard pressure balance equation:

$$\Delta P_c = \Delta P_v + \Delta P_l + \Delta P_g$$

and neglecting, for the purposes of a first approximation, the vapour pressure drop ΔP_v , we can substitute for the pressure terms and obtain

$$\frac{2\sigma_l \cos \theta}{r_c} = \frac{\mu_l}{\rho_l L} \times \frac{Q_{\text{eff}}}{A_w K} + \rho_l g l \sin \phi$$

Rearranging and substituting for \dot{m} , we obtain

$$\dot{m} = \frac{\rho_l K A_w}{\mu_l l_{\text{eff}}} \left\{ \frac{2\sigma_l}{r_c} \cos \theta - \rho_l g l_{\text{eff}} \sin \phi \right\}$$

The wire diameter of 250 mesh is typically 0.0045 cm, and therefore the thickness of two layers of 250 mesh is 4×0.0045 cm or 0.0180 cm.

The bore of the heat pipe is 1 cm.

$$\begin{aligned} \therefore A_{\text{wick}} &= 0.018 \times \pi \times 1 \\ &= 0.057 \text{ cm}^2 \\ &= 0.057 \times 10^{-4} \text{ m}^2 \end{aligned}$$

From Table 3.4, the pore radius r and permeability K of 250 mesh are 0.002 cm and $0.302 \times 10^{-10} \text{ m}^2$, respectively. Assuming perfect wetting ($\theta=0^\circ$), the mass flow \dot{m} may be calculated using the properties of water at 100°C.

$$\begin{aligned} L &= 2258 \text{ J/kg} \\ \rho_l &= 958 \text{ kg/m}^3 \\ \mu_l &= 0.283 \text{ mNs/m}^2 \\ \tau_l &= 58.9 \text{ mN/m} \end{aligned}$$

Converting all terms to the base units (kg, J, N, m and s)

$$\begin{aligned} \dot{m}_{\max} &= \frac{958 \times 0.302 \times 10^{-10} \times 0.057 \times 10^{-4}}{0.283 \times 10^{-3} \times 0.3} \\ &\quad \times \left(\frac{2 \times 58.9 \times 10^{-3}}{0.2 \times 10^{-4}} - 958 \times 9.810 \times 0.3 \times 0.5 \right) \\ &= 1.95 \times 10^{-9} (5885 - 1410) \\ &= 8.636 \times 10^{-6} \text{ kg/s} \\ \dot{Q}_{\max} &= \dot{m}_{\max} \times L \\ &= 8.636 \times 10^{-6} \times 2.258 \times 10^6 \\ &= 19.5 \text{ W} \end{aligned}$$

4.4.3 Solution – Revised Design

Consider the addition of two layers of 100-mesh wick below the original 250 mesh.

The wire diameter of 100 mesh is 0.010 cm
 \therefore Thickness of two layers is 0.040 cm.
 Total wick thickness = 0.040 + 0.018 cm
 = 0.058 cm
 $\therefore A_{\text{wick}} \approx 0.058 \times \pi \times 1$
 $\approx 0.182 \text{ cm}^2$

The capillary pressure is still governed by the 250 mesh, and $r_c = 0.002 \text{ cm}$. The permeability of 100 mesh is used, Langston and Kunz giving a value of $1.52 \times 10^{-10} \text{ m}^2$. The mass flow may now be calculated as:

$$\begin{aligned} \dot{m}_{\text{max}} &= \frac{958 \times 1.52 \times 10^{-10} \times 0.057 \times 10^{-4}}{0.283 \times 10^{-3} \times 0.3} \\ &\times \left(\frac{2 \times 58.9 \times 10^{-3}}{0.2 \times 10^{-4}} - 958 \times 9.810 \times 0.3 \times 0.5 \right) \\ &= 31 \times 10^{-9} (5885 - 1410) \\ &= 139 \times 10^{-6} \text{ kg/s} \\ \dot{Q}_{\text{max}} &= \dot{m}_{\text{max}} \times L \\ &= 139 \times 10^{-6} \times 2.258 \times 10^6 \\ &= 314 \text{ W} \end{aligned}$$

The modified wick structure has resulted in an estimated increase in capacity from 19.5 to 314 W, that is the limiting performance has been improved by more than an order of magnitude. A disadvantage of the additional layers lies in the additional thermal resistance introduced at the evaporator and the condenser.

4.5 THERMOSYPHONS

The design process for a thermosyphon is similar to that for a wicked heat pipe in that it requires identification of suitable case material and working fluid, followed by evaluation of the performance of the unit using the techniques discussed in Chapter 2. The wicking limitation is not relevant to thermosyphon performance. The thermal resistance of any wick used to distribute liquid through the evaporator must, however, be taken into account.

4.5.1 Fluid Inventory

In the case of thermosyphons, the fluid inventory is based on different considerations from wicked heat pipes [5]. The amount of liquid is governed by two considerations; too small a quantity can lead to dryout, while an excess of liquid can lead to quantities being carried up to the condenser, where blockage of surface for condensation can result. Bezrodnyi and Alekseenko [6] recommended that the liquid fill should be at least 50% of the volume of the evaporator and also that the volume of liquid, V_l , should be related to the thermosyphon dimensions as follows:

$$V_l > 0.001 D(l_e + l_a + l_c)$$

where D is the pipe's internal diameter.

When a wick is fitted to the evaporator section, ESDU [7] recommends

$$V_l > 0.001 D(l_a + l_c) + A_w l_e \varepsilon$$

where ε is the wick porosity.

Comprehensive work by Groll et al. at IKE, Stuttgart, investigated the effect of fluid inventory on the performance of thermosyphons incorporating a variety of novel liquid–vapour flow separators (to minimise interaction between these components). It was found, for several working fluids [8], that the fluid inventory, expressed as a percentage of the evaporator volume occupied by the liquid working fluid, had a rather flat optimum between about 20% and 80%.

The constraints on filling for a closed two-phase thermosyphon are illustrated by El-Genk and Saber [9]. Low initial filling ratio results in dryout of the evaporator, while excess working fluid results in liquid filling the entire evaporator when bubbles form due to boiling.

4.5.2 Entrainment Limit

The third limit shown in Fig. 4.6 is the entrainment or counter current flooding limit discussed in Section 2.4.2.

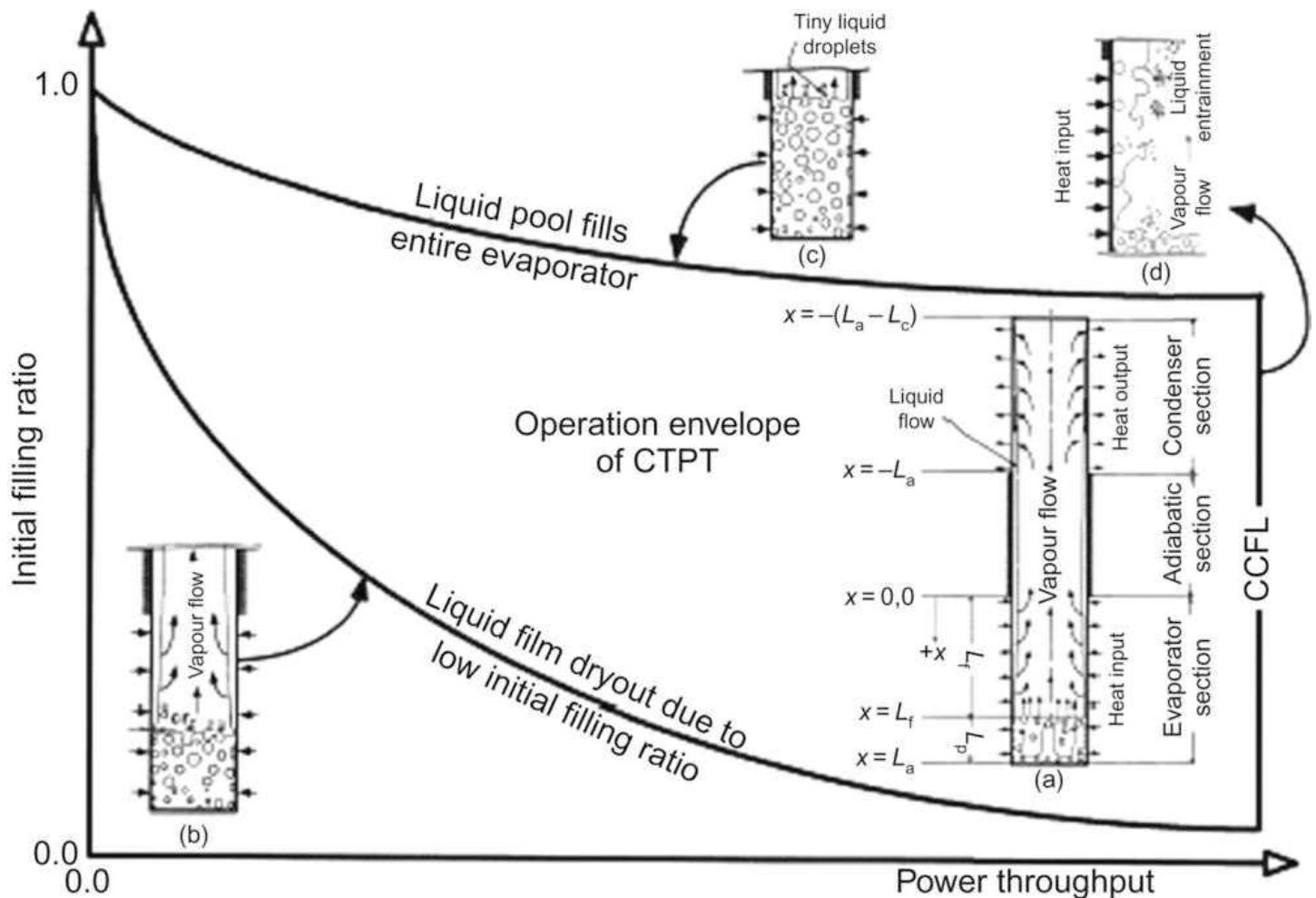


Figure 4.6: Operating envelope of closed two-phase thermosyphons (CTPT) [9]

4.6 SUMMARY

In this chapter, the theory presented in Chapter 2 and the practical considerations of material and working fluid choice described in Chapter 3 have been used to illustrate the process of designing simple wicked heat pipes. The design of thermosyphons uses similar techniques, but the important differences have been highlighted.

REFERENCES

- [1] B.D. Marcus, Theory and design of variable conductance heat pipes, TRW Systems Group, NASA CR-2018, April 1972.
- [2] H.R. Holmes, A.R. Field, The gas-tolerant high capacity tapered artery heat pipe, in: AIAA/ASME Fourth Joint Thermophysics and Heat Transfer Conference, Paper AIAA-86-1342, Boston, MA, 1986.
- [3] Anon, ASHRAE Handbook of Fundamentals, ASHRAE, 2005, p. 20.35.
- [4] W.H. McAdams *Heat Transmission* third ed. 1954 McGraw-Hill
- [5] Anon, Heat pipes – performance of two-phase closed thermosyphons, Data – Item No. 81038, Engineering Sciences Data Unit, London, 1981.
- [6] M.K. Bezrodnyi D.B. Alekseenko *Investigation of the critical region of heat and mass transfer in low temperature wickless heat pipes High Temp.* 15 1977 309–313
- [7] Anon, Heat pipes – general information on their use, operation and design, Data Item No. 80013, Engineering Sciences Data Unit, London, 1980.
- [8] M. Groll, H. Nguyen-Chi, H. Krahling, Heat recovery units employing reflux heat pipes as components, Final Report, Contract EE-81-133D(B), Commission of the European Communities Report EUR9166EN, 1984.

[9] M.S. El-Genk H.H. Saber *Determination of operation envelopes for closed/two-phase thermosyphons* *Int. J. Heat Mass Transf.* 42 1999 889–903